Egypt.J.Chem. **Vol. 63**, No.9. pp. 3179- 3190 (2020)

Egyptian Journal of Chemistry
http://ejchem.journals.ekb.eg/

Removal of Methylene Blue from Aqueous Solutions by Magnetic Acrylic Acid-co-butyl Methacrylate

R. E. Khalifa[1*], A. Ghozlan[2], H. Abd El-Wahab[3]

[1]Polymer Materials Research Department, Advanced Technologies and New Materials Research Institute (ATNMRI), City of Scientific Research and Technological Applications (SRTA-City), New Borg El-Arab City, P.O. Box: 21934 Alexandria, Egypt.

[2]Leader for Chemical Industries and Cosmetics Company

[3]Chemistry Department, Faculty of Science, Al-Azhar University, Egypt.

IN this study, a polyacrylic acid-co-butyl methacrylate/Fe_3O_4 nanocomposite was prepared using in-situ coprecipitation polymerization technique, for the adsorptive removal of methylene blue (MB) dye from industrial wastewater. Chemical structure of the prepared magnetic nanocomposite was confirmed using Fourier transform infrared spectroscopy (FTIR). Thermal properties were studied using thermal gravimetric analysis (TGA), while the morphological structure was examined using a scanning electron microscope (SEM). Different parameters affecting the adsorption process, such as contact time, pH, adsorbent dosage, agitation speed, and initial dye concentration, were also studied. This study indicated that the percentage removal of MB dye has decreased with increasing initial dye concentration while increased with raising the agitation speed from 100 to 300 rpm. Additionally, studying the pH profile of the dye solution shows that the highest MB removal percentage (98%) was recorded at pH 3.5. These results demonstrated that the prepared magnetic nanocomposite could be considered as a promising adsorbent for the removal of MB dye from industrial wastewater.

Keywords: Polyacrylic acid, In-situ coprecipitation polymerization, Adsorption, Wastewater, Removal percentage (%).

Introduction

Up to date, water pollution considered one of the worst environmental problems as a result of the continual discharge of toxic and hazardous chemicals to the environment [1]. The presence of dyes residues in the effluents from many industries such as paper, textile, plastics, leather, rubber, pharmaceutical, food industries, and cosmetics, has a primary environmental concern [2, 3]. This discharge has adverse effects on health, marine lives, global ecosystems, and microbial population's. Accordingly, the presence of little dye concentrations (<1ppm) in the industrial effluent is highly undesirable and visible. Currently, there are about 10,000 available commercial types of pigments and dyes with annual production rate over 7x105 tones worldwide [4, 5]. Methylene blue (MB) is the most commonly used constituent for dyeing cotton, silk, and wood. It can cause severe problems as permanent injury to the eyes, breathing difficulties, vomiting, nausea, mental confusion, profuse sweating, and methemoglobinemia [6]. Therefore, the treatment of wastewater containing such dye is of a matter of great interest [7].

During the past decades, several chemicals, physical and biological decolourisation techniques have been stated. Numerous treatment processes have been used for removing dyes from wastewater streams such as photo-catalytic degradation, sonochemical degradation, and electrochemical degradation. Besides, cation exchange membranes, micellar-enhanced ultrafiltration, electro-coagulation, adsorption processes, integrated chemical–biological degradation, integrated iron (III) photo-assisted

*Corresponding author e-mail: randaghonim@gmail.com
Received 2/1/2020; Accepted 30/4/2020
DOI: 10.21608/ejchem.2020.21821.2300

biological treatment, and Fenton biological treatment [8] were also used. Adsorption is well-known effective separation methods for water reuse applications [9]. Adsorption is superior to other systems for water decontamination in terms of cost, simplicity, flexibility, ease of operation [10]. It also does not result in the formation of harmful by-products. Recently, many approaches have been focused on the development of non-conventional, cheaper, and effective adsorbents, including natural materials, bio-sorbents, and waste materials from industry and agriculture [11-12]. Using numerous polymers with different functional groups has attracted considerable attention because of their high adsorption capacities, reuse for continuous processes and regeneration abilities. Over the past decade, organic-inorganic nanocomposite polymers have attracted extensive consideration owing to their exceptional property with the grouping of both inorganic nanoparticles and organic polymer [13-16]. For magnetic adsorption, it is critical to select the suitable nanoparticles (NPs) with a high adsorption capability [17-18]. The incorporation of magnetic nanoparticles such as iron oxide NPs into a polymeric matrix can create tunable nanocomposite that can be remotely controlled by a magnetic field. The present work aims to study the applicability of the synthesised poly (acrylic acid-co-butyl methacrylate/Fe3O4) nanocomposite for the adsorption of methylene blue from dying water. Accomplished nanocomposite was characterized by FTIR, TGA, and SEM analysis. The effect of several factors affecting adsorption efficiencies such as contact time, initial MB concentration, agitation rate, pH, and adsorbent dose have been studied.

Materials and Methods

Materials

Ferric chloride (Mw=162.2 g/mol; purity 99%) and hydrated ferrous chloride (purity 98%; Mw=126.751g/mol) was obtained from LOPA Chemi Mumbai (India). Ammonia solution (Mw=35.04 g/mole; purity 33 %), Methanol (purity 99%), 1-propanol (purity 99), and 2-propanol (purity 99%) were supplied from El-Nasr company, Alexandria (Egypt). Citric acid was purchased from Eastern fine chemicals Co (Cambodia). Potassium persulphate (KPS; purity 99%) and acetone (purity99%) were purchased from Sigma-Aldrich (Germany). Ethanol (purity 99.8%) was obtained from Labtech for chemical reagents (India). Butyl methacrylate, stabilized (MW=142.2 g/mole; purity 99.8%; density= 0890 g/ml) and acrylic acid, stabilized (Mw= 72.06 g/mole; purity 99.5%; density= 1.05 g/ml) were obtained from Acros organics, Geel (Belgium). MB (basic blue 9, chemical formula, $C_{16}H_{18}ClN_3S{\cdot}3H_2O$; MW, 373.90 g/ mol) was purchased from Carlo Erba. All chemicals were used without further purification.

Methods

Preparation of iron oxide nanoparticles

Iron oxide nanoparticles were prepared using the co-precipitation method [19]. In brief, 200 g of $FeCl_3.6H_2O$ was dissolved in 1250 mL distilled water, and 100 g of $FeCl_2.4H_2O$ was dissolved in 2500 mL distilled water. The two solutions were mixed in a 5-litre beaker; then the temperature was elevated to 80 °C under stirring in a free oxygen atmosphere. 975 mL of ammonia solution 33 % was added dropwise to adjust pH in the range of 8-9. After that; the solution kept under stirring for 2 hr. 500 mL citric acid solution (2M) was added to the reaction mixture to prevent coagulation of the formed magnetic nanoparticles, the settlement was allowed to cool, and the precipitate was settled in the bottom of the beaker. The produced iron oxide nanoparticles were separated via centrifugation at 4000 rpm and washed with distilled water several times. The nanoparticles were dried at 100°C for 2 hr.

Preparation of polymer nanocomposite

Poly (acrylic acid-co-butyl methacrylate/Fe_3O_4) nanocomposite was synthesised by the in-situ co-precipitation polymerisation method. According to this method, butyl methacrylate (BMA) was added to acrylic acid (AA) with the composition of (70:30 %wt.). The two monomers were dissolved in co-solvents of ethanol and water with a solvent composition of (50:50) in a conical flask. 2.5 mM $K_2S_2O_8$ was added to the reaction mixture with 0.1g of the prepared iron oxide nanoparticles. The reaction mixture was then placed into a water bath shaker at 60 °C and 100 rpm for 4 hr. A white precipitate indicates the formation of copolymers. The solution was then allowed to cool for 24 hrs, washed three times with hot distilled water, and then centrifuged at 4000 rpm to remove any unreacted monomers. The precipitate was dried at 70 °C for 48 hrs. Finally, the obtained nanocomposite was ground in a blender and sieving using molecular sieves to obtain a uniform particle size before use.

Batch adsorption process

All batch adsorption experiments were carried out using a pre-weighed sample of the synthesized nanocomposite adsorbent in addition to a known volume of MB solution. The dye solution was prepared by dissolving specific weight of MB in distilled water. Then, the mixture was shacked at a shaking rate of 120 rpm/min. All experiments were conducted using different contact time (10, 20, 30, 40, 60, 90, 150 and 210) min, adsorbent dosages (0.25, 0.4, 0.8 and 1) g/50 mL of dye solution, initial MB concentration (10, 25, 50, 60, and 100) mg/L, temperature (25, 35, 45 and 55) °C, agitation rate (100, 200, 300 and 400) rpm, and pH of the solution (3.5, 7, 9 and 11). The pH was adjusted by adding aqueous solutions of HCl or NaOH (0.1 mol/L). The remaining dye concentration was determined at λ_{max} = 668 nm using UV–visible spectrophotometer (Pharmacia Biotech). The removal percentage (%) and adsorption capacity of dye molecules was calculated according to the following equation [20]:

$$\%\text{Removal} = \frac{C_o - C}{C_o} \times 100 \qquad (1)$$

$$q = \frac{(C_o - C)V}{W} \qquad (2)$$

Where C_o is the initial dye concentration (mg/L) and C_t is the residual dye concentration (mg/L). V is the solution volume (L) and W is the adsorbent weight (g).

Characterization

Superconducting quantum interference device (SQUID) magnetometer was used to determine magnetic properties of the prepared iron oxide nanoparticles and polymer nanocomposite. Chemical characteristics of the fabricated poly (acrylic acid-co-butyl methacrylate/Fe_3O_4) nanocomposite were investigated by Fourier-transform infrared (FT-IR) spectroscopy (Shimadzu FTIR - 8400 S- Japan). While, the surface morphologies of the synthesised nanocomposite were observed with a scanning electron microscope (SEM, Joel Jsm 6360LA-Japan). Also, the thermal stability was also studied in a temperature range of 20-600 °C using thermo gravimetric analyzer (ShimadzuTGA–50, Japan under nitrogen at a flow rate of 20 mL/min and at a heating rate of 10 °C/min.

Results and Discussion

Magnetic properties analysis

The super paramagnetic behavior is an important feature of the prepared nanocomposite Fe_3O_4 nanoparticles. Figs.1a&b. show the matter magnetization variations for the prepared iron oxide nanoparticles and the polymer nanocomposite. Magnetic field of the Fe_3O_4 nanoparticle, magnetic features such as magnetization saturation (M_s), field reversals (H_c), and residual magnetization (M_r) depend on a magnetic nanoparticle's size and shape. The magnetization curve of Fe_3O_4 nanoparticles, which were obtained in isothermal magnetic conditions at room temperature, is illustrated in Fig. 1a. It is clear from the figure that Fe_3O_4 nanoparticles have super paramagnetic properties due to the small amount M_r present. The hysteresis loops show super paramagnetic behavior for Fe_3O_4 nanoparticles. The saturation magnetization (M_s) values were 65.11 emu·g^{-1} Fe_3O_4. Fig.1b. show the matter magnetization variations based on the magnetic field of the Fe_3O_4 nanoparticle. Magnetization curve shown in Fig.1b confirm that the polymer nanocomposite have magnetic properties due to the presence of magnetic Fe_3O_4. Table 1 shows comparing M_s, M_r, and H_c in iron oxide nano particles and polymer nanocomposite.

Fourier transforms infrared spectroscopy (FTIR)

The FT-IR spectrum of the prepared nanocomposite was presented in Fig.2. It was observed from the figure that the broadband appears at 3292 cm^{-1} was related to the stretching vibration of OH. Also, Methyl groups were identified by the weak peak at 2958.90 cm^{-1}. The typical broadband appears at 1728.28 cm^{-1} may be attributed to carbonyl-stretching vibration. Additionally, the absorption band at 1161.19 cm^{-1} was assigned to the characteristic vibration of C=O group in the carboxylic acid. Further, an absorption peak appeared at 532 cm^{-1}, indicated Fe-O stretching vibration in the Fe_3O_4 nanoparticles [21].

Thermal gravimetric analysis (TGA)

The thermal stability of the prepared magnetic nanocomposite was illustrated in Fig 3. It was demonstrated that there are three decomposition steps for the thermal degradation of poly (acrylic acid-co-butyl methacrylate/Fe_3O_4) nanocomposite, namely; dehydration, decarboxylation and chain scission [22]. In the first stage (26.97 -100.04 °C), there was a small decrease in the polymer nanocomposite weight about 0.202 %, due to the evaporation of the adsorbed moisture. The slow rate of evaporation may be attributed to the presence of magnetic

iron nanoparticles which shift the dehydration temperature to higher temperature in the range of 100.04 to 293.74 °C. In the second stage (100.04-293.74 °C), a weight loss of 4.224% was occurred due to the evaporation of the weak physically and strong chemically bounded water. On the other hand, the third step (293.75-436.20 °C) exhibited a significant decrease in the polymer nanocomposite weight (88.320 %); this may be regarded to the decarboxylation reaction throw the thermal degradation and also for the formation of anhydrides which take place between 293.75 and 350 °C. The majority of these anhydrides involve the formation of six-membered glutaric anhydride rings by the reaction of adjacent acid groups [23]. Besides, the decomposition of the carboxylic group to carbon dioxide becomes increasingly important above 350 °C, and both water and carbon dioxide continues to be evolved on heating up to 500 °C. Chain scission occurred at a temperature above 350-436.20 °C, where the formation of necessary amounts of cold ring fraction consisting of the dimer, trimer, etc. was possible owing to the release of fragments with short sequences of acrylic acid. Finally, about 1.635 % depression in poly (acrylic acid-co-butyl methacrylate/Fe_3O_4) nanocomposite weight occurred in the fourth stage between 436.20 and 599.89 °C owing to the evaporation of the reminder amounts of CO_2 and water. The results

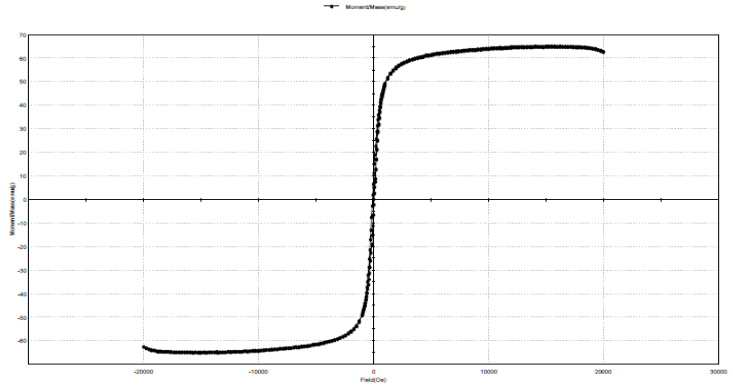

(a)

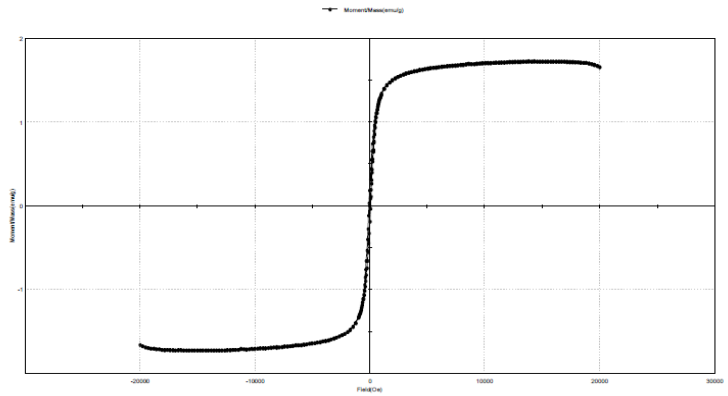

(b)

Fig. 1. magnetization variations for the Fe3O4 nanoparticles and prepared nanocomposite at room temperature.

TABLE 1. Comparing Ms, Mr, and Hc for iron oxide nano particles and the prepared nanocomposite.

Sample	Ms (emu/g)	Mr (emu/g)	Hc (Oe)
Magnetic iron oxide	65.113	6.455	72.547
Magnetic nanocomposite	1.725	0.189	61.814

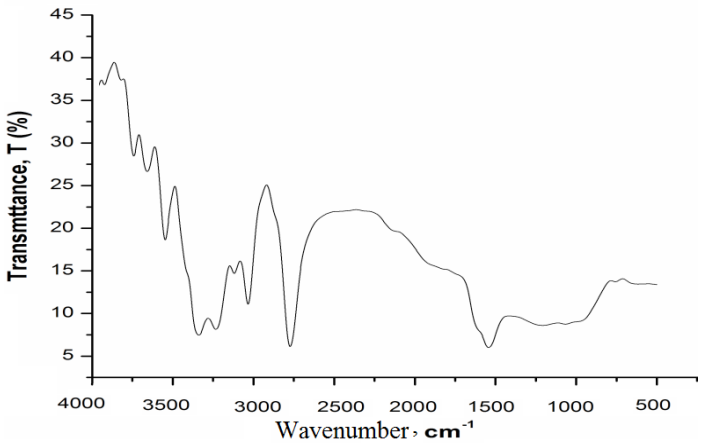

Fig. 2. FTIR spectra of poly (acrylic acid-co-butyl methacrylate/Fe3O4) nanocomposite.

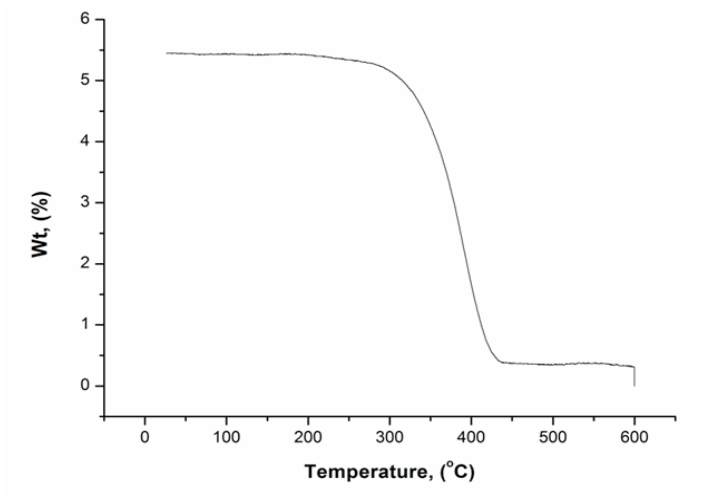

Fig. 3. TGA of poly (acrylic acid-co-butyl methacrylate/Fe_3O_4) nanocomposite.

also indicated that the T_{50}% where the fabricated magnetic nanocomposite loss their half weight is 383.39 °C, which confirms the thermal stability of the prepared magnetic nanocomposite.

Scanning electron microscope (SEM)

Morphological analysis of the synthesized magnetic nanocomposite was described in Fig 4. The images show a regular distribution of spherical particles of the copolymer of the hydrophilic AA which obtained easily without the use of any cross-linker as an advantage of the precipitation polymerization technique [24] with the almost homogenous distribution.

Factors affecting adsorption process

Effect of contact time

The impact of contact time was evaluated to establish the equilibrium time for the maximum MB removal using the prepared magnetic nanocomposite adsorbent as shown in Fig 5. The results illustrated that there was an increase in the removal % by increasing contact time starting from 10 min till the maximum value of 96.44 % at 210 min. However, the removal efficiency remains constant with further increase in time. This effect may be initiated due to, the large concentration gradient between the liquid phase and the solid surface besides; more active sorptive sites are also available. Thus, the diffusion onto the external surface, which is followed by pore diffusion into the intraparticle matrix, is faster up to attain the equilibrium at 210 min [25]. Eventually, when the time goes by, binding sites in the adsorbent are not available for further adsorption of the dye molecules due to the deposition of dyes on the available active sites on the adsorbent [26, 27]. At this point, the amount of dye desorbing from

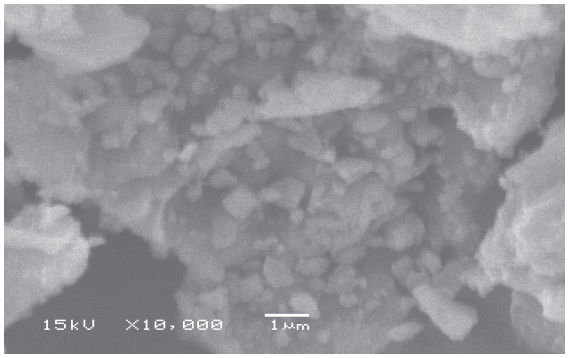

Fig. 4. SEM image of poly (acrylic acid-co-butyl methacrylate/Fe_3O_4) nanocomposite.

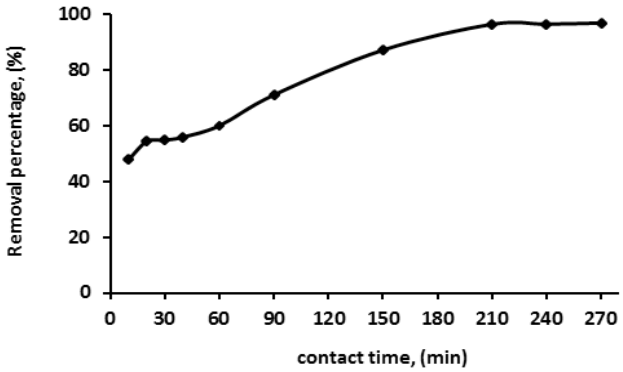

Fig. 5.Effect of contact time on the MB removal % using 0.25g of poly (acrylic acid-co-butyl methacrylate/ Fe3O4) nanocomposite, 25 mg/L, agitation rate 300 rpm, at 25 °C.

the adsorbent is in a state of dynamic equilibrium with the amount of dye being adsorbed onto the adsorbent. These observations agreed with the other published results [25,28].

Effect of initial dye concentration

The initial adsorbate concentration in the solution provides an important driving force in overcoming mass transfer resistance between the aqueous and the solid phases [29]. Equilibrium adsorption studies was performed to determine the removal percentage % of the adsorbent, and the equilibrium is established when the concentration of adsorbate in the bulk solution is in dynamic balance with that on the surface [30]. Fig 6 shows the effect of inititial MB concentration on the removal efficeny onto poly (acrylic acid-co-butyl methacrylate/Fe_3O_4) nanocomposite. It was clear that there was a decrease in the MB removal % with increasing the initial dye concentration, this result was expected as at lower concentration large surface area was available for MB cations but, as the concentration increased the active sites become blocked and saturated. This trend may be due to the electrostatic repulsive forces between the solid and bulk phase[31-33].

Effect of agitation rate

Fig. 7 shows the impact of agitation rate on the removal of MB molecules onto the synthesiesd nanocomposite. It was indicated that increasing the agittaion speed from 100-300 rpm resulted in an increase in the adsorption effiecncy. This observation may be regarded to the improve in the collisions between dye molecules and the solid particles with the raise in the agiation rates, which lead to an increase in the amount of dye adsorbed on the binding sites of the adsorbent [25]. In contrast, raising the speed above 300 rpm has not significant effect on the removal % due to the saturation of active sites, also the desorption begins to take place and dye ions begins to transport slowly from the solid phase into the liquid [34].

Effect of adsorbent dosage

Figure 8 domenstrates the effect of adsorbent dosage on the adsorption process of MB dye at fixed initial dye concentration with shaking until equilibrium [35]. The figure reveals that increasing the adsorbent dose from 0.1 to 0.4 g has a positive effect on the % removal. These results may be due to the increase in the adsorption surface

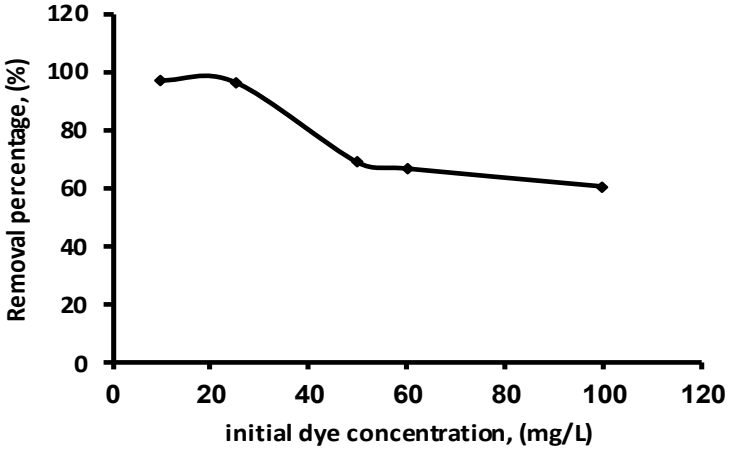

Fig. 6. Effect of initial dye concentration on the MB removal % using using 0.25g of poly (acrylic acid-co-butyl methacrylate/Fe3O4) nanocomposite, agitation rate 300 rpm, at 25 °C for 4 hr.

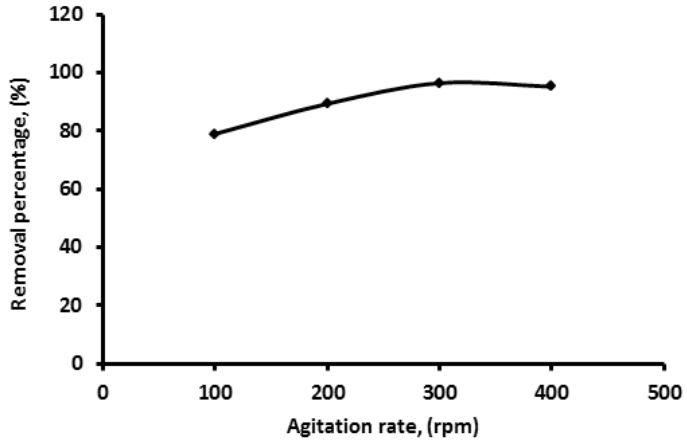

Fig.7. Effect of agitation rate on the MB removal % using 0.25g of poly (acrylic acid-co-butyl methacrylate/ Fe3O4) nanocomposite, 25 mg/L, at 25 °C for 4 hr.

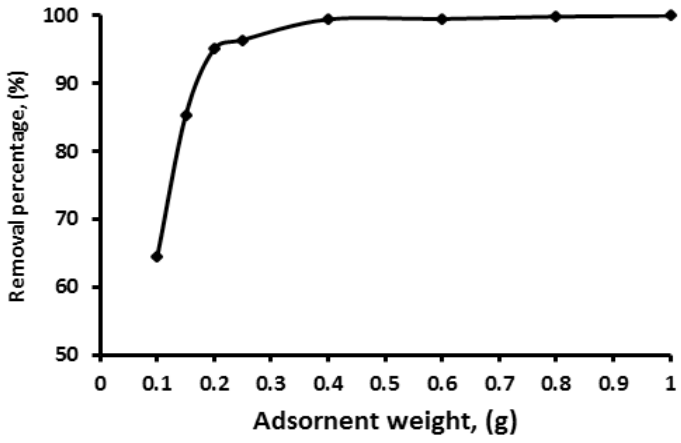

Fig. 8. Effect of adsorbent dosage on the MB removal %, (25 mg/L, agitation rate 300 rpm, at 25 °C for 4 hr).

area along with the presence of more active sites [36,37]. While there is no signeficant increcrase in the removal % above 0.3 g owing to the saturation of the vacnt active sites till the plateau.

Effect of pH

One of the most important factors affecting the efficency of adsorbent in wastewater treatments is the solution pH. The efficiency of adsorption should be depends on the solution pH, since variation in pH leads to the variation in the degree of ionization of the adsorptive molecule and the surface properties of adsorbent [38]. Fig. 9 shows that the the highest MB removal % was at pH 3.5 due to the electrostatic interaction between the cationic dye molecules and the negative charges on the surface of adsorbent. Additionally, at pH 7 the MB removal % reduced while a insignificant increase was observed at pH 9. This behaviour occurred beacuse with increasing the pH above the pKa of the poly(acrylic acid) (pKa=4.2), the excess H^+ ions present in the solution began to compete with dye molecules for the adsorption sites [39,40]. Hence, again at pH 11 the MB removal % decline due to the saturation of adsorbent sites and the occurrence of desorption of adsorbed ions.

Equilibrium study

Adsorption isotherms are used to explicate the nature of adsorption and interaction between quantity adsorbed and initial dye concentrations, as well as the existing equilibrium between adsorbent and adsorbate [26]. Therefore, adsorption isotherms are critical in optimizing the use of adsorbents. In this research, two well-known adsorption isotherm shapes have used to fit the experimental data. The linear equation of Langmuir (Eq.3) and Freundlich (Eq.4) are given as [30]:

$$\frac{C_e}{q_e} = \frac{1}{q_{max} K_L} + \frac{C_e}{q_{max}} \quad (3)$$

$$\ln q_e = \ln K_F + \frac{1}{n} \ln C_e \quad (4)$$

Where q_{max} (g/g), C_e (g/L), and K_L (L/g) are the saturated adsorption capacity, the dye concentration at equilibrium, and the Langmuir isotherm constant, respectively, 1/n and K_f are the Freundlich constants belonged to adsorption intensity and adsorption capacity.

The two isotherms are portrayed in Fig.10 a&b, the isotherm constants whose values signify the perceptivity of the adsorbate toward the surface of adsorbent are shown in Table 2. The values of q_{max} and the low values of K_L obtained from the linear plot of the Langmuir model (Fig. 10a), illustrates that the synthesized nanocomposite have a high affinity for MB dye molecules [41]. Otherwise, the values of the dimensionless separation factor (R_L) are mentioned in Table 3, which outline the fundamental characteristics of the Langmuir isotherm were $0 < R_L < 1$ and the values of n were greater than 1, demonstrating the favorable adsorption of MB dye on the synthesized adsorbents. This suggests that the prepared nanocomposite is a suitable adsorbent for dye molecules. In addition, the R^2 values for both the Langmuir and the Freundlich isotherms are

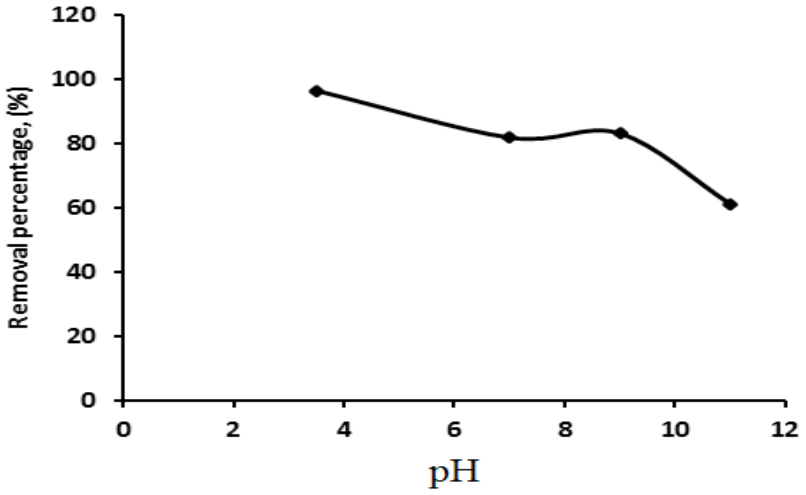

Fig. 9. Effect of pH on the MB removal % using 0.25g of poly (acrylic acid-co-butyl methacrylate/Fe3O4) nanocomposite, 25 mg/L, agitation rate 300 rpm, at 25 °C for 4 hr.

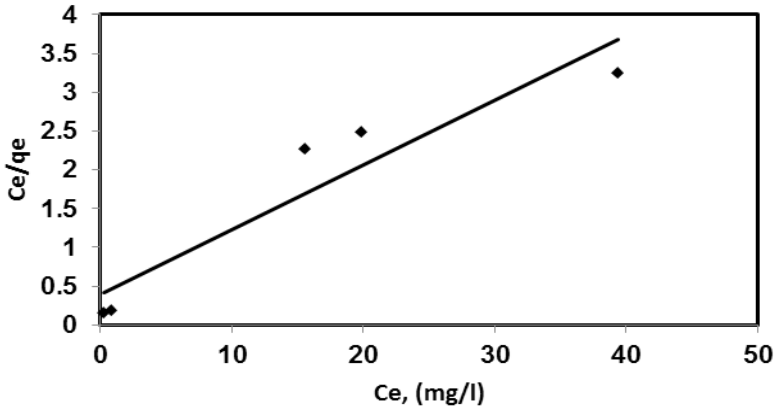

(a)

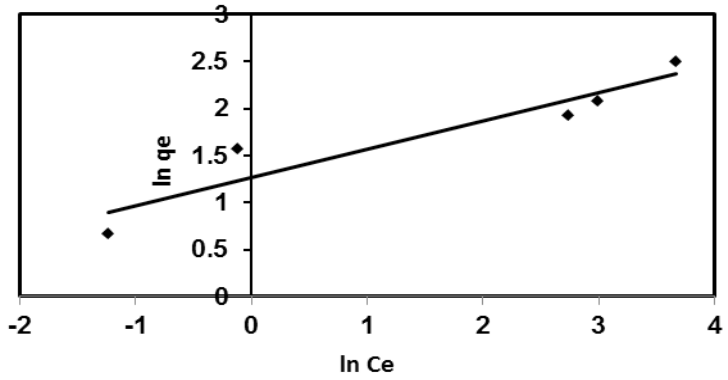

(b)

Fig. 10. Equilibrium isotherm for the adsorption of MB onto poly (acrylic acid-co-butyl methacrylate/Fe3O4) nanocomposite; (a) Langmuir and (b) Freundlich isotherm.

TABLE 2. Langmuir parameters for the adsorption of MB on acrylic acid-co-butyl methacrylate/Fe_3O_4) nanocomposite

Isotherm model	Parameters	Values
Langmuir	q_{max} (mg/g)	12.00
	K_L (L/mg)	0.18
	R^2	0.89
Freundlich	K_f(mg/g)	3.53
	1/n	0.30
	R^2	0.89

TABLE 3. the dimensionless separation factor (R_L) for acrylic acid-co-butyl methacrylate/Fe_3O_4) nanocomposite at different MB initial concentrations,

MB initial concentration (mg/L)	R_L
10	0.003309
25	0.001326
50	0.000663
60	0.000553
100	0.000332

similar and close to 1, describing that monolayer and multilayer adsorption played a very important role in the dye removal process. The maximum monolayer adsorption capacity was obtained to be 12.9 mg/g.

Conclusion

Adsorption study had been carried out for the removal of the methylene blue dye (MB) from wastewater using poly (acrylic acid-co-butyl methacrylate/Fe_3O_4) nanocomposite which synthesized by in-situ co-precipitation polymerization method via free radical polymerization. The prepared adsorbent was characterized by VSM, FTIR, TGA, and SEM. The effect of numerous factors on the removal % was also investigated. The results revealed that the equilibrium is prictaclly achieved at 210 min. It was also indicated that the MB removal (%) decreased with the increase in the initial MB concentration, and increase with raising the agitation speed from 100 to 300 rpm. Additionally, studying the pH effect shows that the highest MB removal percentage (%) was occurred at pH 3.5. In addition, the equilibrium study confirms that the adsorption of MB onto the prepared nanocomposite followed both Langmuir and Freundlich isotherm with maximum monolayer adsorption capacity 12 mg/g. The separation factor (RL) of the Langmuir and the exponent (n) of the Freundlich indicated the favorability of adsorption of MB from aqueous solution. In conclusion, the fabricated magnetic nanocomposite could be used efficiently in the adsorption of the methylene blue dye from wastewater.

References

1. Do J.S., and Chen M.L., Decolourization of dye containing solutions by electrocoagulation, *Journal of Applied Electrochemistry*, **24**, 785-790, (1990).
2. Ahmad A., Mohd-Setapar S. H., Chuong C. S., Khatoon A., Wani W. A., Kumar R. and Rafatullah M., Recent advances in new generation dye removal technologies: novel search for approaches to reprocess wastewater, *Royal Society of Chemistry Advances*, **5**, 30801–30818(2015).
3. Yagub M. T., Sen T. K., Afroze S. and Ang H. M., Dye and its removal from aqueous solution by adsorption: A review, *Advances in Colloid and Interface Science*, **209**, 172–184(2014).
4. Helmer R. and Hespanhol I., Water pollution control-a guide to the use of water quality management principles, *E & FN Spon, London*, (1997).
5. Lehr J. H., Gass T. E. and Pettyjohn W. Domestic water treatment, *McGraw-Hill Book Company*, New York, , (1980).
6. Guo R., Wilson L.D., Synthetically engineered chitosan-based materials and their sorption properties with methylene blue in aqueous solution, *Journal of colloid and interface science*, 388, 225–234(2012).
7. Liu S., Zhang A., Yan K., Ye Y. and Chen X., Microwave-enhanced catalytic degradation of methylene blue by porous MFe2O4 (M= Mn, Co) nanocomposites: Pathways and mechanisms, *Separation and Purification. Technology*. 135, 35–41(2014).
8. Mohammed M.A., Shitu A. and Ibrahim A., Removal of methylene blue using low cost adsorbent: A review, Research Journal of Chemical Sciences, 4(1), 91-102 (2014).
9. Dabrowski A., Adsorption-from theory to practice. Advances in Colloid and Interface Science. 93(1-3), 135–224 (2001).
10. Othman S., Noor S.G., Mohd R., and Rokiah H., Removal of Zn(II) and Cd(II) ions from aqueous solutions using Surfactant Modified Bamboo Sawdust. Separation Science and Technology, 46(14), 2275–2282(2011).
11. Ahmad A., Rafatullah M., Sulaiman O., Ibrahim M.H., Chii Y.Y. and Siddique B.M., Removal of Cu(II) and Pb(II) ions from aqueous solutions by adsorption on sawdust of Meranti wood, *Desalination*, 247(1), 636–646 (2009).
12. Abd-Elhamid A. I., El Fawal G.F., Akl M.A., Methylene blue and crystal violet dyes removal (as a binary system) from aqueous solution using local soil clay: kinetics study and equilibrium isotherms. *Egyptian Journal of Chemistry*. (2018).
13. Okada A. and Usuki A., Twenty years of polymer clay nanocomposites. *Macromolecular Material Engineering*. 291, 1449-1476 (2006).
14. Tamer T. M., Abou-Taleb W. M., Roston G. D., Mohyeldin M .S. , Omer A. M. , Khalifa R. E. and Hafez A.M., Formation of zinc oxide nanoparticles using alginate as a template for purification of wastewater, *Journal of Environmental Nanotechnology, Monitoring & Management*, 10, 112-121(2018).

15. M. S. Mohy Eldin, M. H. Abd Elmageed, A. M. Omer, T. M. Tamer, M. E Yossuf, R. E. Khalifa, Novel Aminated Cellulose Acetate Membranes for Direct Methanol Fuel Cells (DMFCs), *International Journal of Electrochemical Science*, 12 (2017) 4301-4318.

16. M. S. Mohy Eldin, M. H. Abd Elmageed, A. M. Omer, T. M. Tamer, M. E Yossuf, R. E. Khalifa, Development of Novel Phosphorylated Cellulose Acetate Polyelectrolyte Membranes for Direct Methanol Fuel Cell Application, *International Journal of Electrochemical Science*,11 (2016) 3467- 3491.

17. Ayman A., Magda A.A., AbdElfatah M.Y. and Mohamed A. I., Superparamagnetic core-shell polymeric nanocomposites for efficient removal of methylene blue from aqueous solutions, *Adsorption Science & Technology*, 31(5), 397-419 (2013).

18. Wei W., Zui D., Minhan C., Haitao J., Zhiqiao Z., Feng L.J. and Ping L., Synthesis and high-efficiency methylene blue adsorption of magnetic PAA/MnFe2O4 nanocomposites. *Applied Surface Science*, 346, 348–353 (2015).

19. Farahmandjou M. and Soflaee F., Synthesis and characterization of α-Fe2O3 nanoparticles by simple coprecipitation Method, *Physical Chemistry Research*, 3(3), 191-196(2015).

20. Liu R.L., Liu Y., Zhou X.Y., Zhang Z.Q., Zhang J. and Dang F.Q., Biomass-derived highly porous functional carbon fabricated by using a free-standing template for efficient removal of methylene blue, *Bioresource Technology*. 154, 138–147 (2014).

21. Didehban K. H., Mohammadi L. and Azimvand J. Preparation of RGO/Fe_3O_4/poly (acrylic acid) hydrogel nanocomposites with improved magnetic, thermal and electrochemical properties, *Materials Chemistry and Physics*, 195, 162-169 (2017).

22. Gaugh M.C. and Kottle S. The thermal degradation of poly(acrylic acid), *Journal of Polymer Science Part B: Polymer Letters,* 5(9), 817-820 (1967).

23. Behnaz H., Sui R. and Charpentier P.A. Synthesis of TiO2/PAA nanocomposite by RAFT polymerization, *Polymer*, 48, 5850-5858(2007).

24. Li G.L, Möhwald H. and Shchukin D.G, Precipitation polymerization for fabrication of complex core-shell hybrid particles and hollow structures, *Chemical Society Reviews*, 42, 3628-3646(2013).

25. Randa E. K., Ahmed M. O., Tamer M. T., Waheed M. S. and Mohamed S. M.E., Removal of methylene blue dye from synthetic aqueous solutions using novel phosphonate cellulose acetate membranes: adsorption kinetic, equilibrium, and thermodynamic studies. *Desalination and Water Treatment*, 144, 272–285 (2019).

26. Elmasry M., Omer A.M., Tamer T. M., Khalifa R. E., Goudaam M. and Mohy Eldin M.S., Removal of methylene blue dye from synthetic aqueous solutions using dimethylglyoxime modified amberlite IRA-420: kinetic, equilibrium and thermodynamic studies, *Desalination and Water Treatment*,144,272-285 (2019).

27. Srivastava V. and Sillanpää M, Synthesis of malachite clay nanocomposite for rapid scavenging of cationic and anionic dyes from synthetic wastewater. *Journal of Environmental Science*, 51, 97-110 (2017).

28. Ahmed M. O., Randa E. K., Tamer M. T., Ahmed A. A., Yossry A. A., Mohamed S. M. E.., Fabrication of a novel low-cost superoleophilic nonanyl chitosan-poly (butyl acrylate) grafted copolymer for the adsorptive removal of crude oil spills. *International Journal of Biological Macromolecules*, 140, 588-599 (2019).

29. Auta M. and Hameed B.H, Coalesced chitosan activated carbon composite for batch and fixed-bed adsorption of cationic and anionic dyes. *Colloids and Surfaces B: Biointerfaces*, 105, 199-206(2013).

30. Omer A.M., Elgarhy G. S. El-Subruiti G.M., Khalifa R.E. and Eltaweil A.S. Fabrication of novel iminodiacetic acid-functionalized carboxymethyl cellulose microbeads for effi-cient removal of cationic crystal violet dye from aqueous solutions, *International Journal of Biological Macromolecules,* 148, 1072-1083(2020).

31. Argun M.E. Activation of pine cone using Fenton oxidation for Cd (II) and Pb (II) removal. *Bioresource technology*, 99(18), 8691-8698(2008).

32. Dog˘an M., Alkan M., Demirbas O. Ozdemir Y. and Ozmetin C. Adsorption kinetics of maxilon blue GRL onto sepiolite from aqueous solutions, *Chemical Engineering Journal*, 124, 89 (2006).

33. Z. Bouberka, A. Khenifi, N. Benderdouche, Z.

Derriche, Removal of Supranol Yellow 4GL by adsorption onto Cr-intercalated montmorillonite, *Journal of Hazards Materials*, 133, 154-161 (2006).

34. Alireza B., Jun T. and Gordon M., Standardization of oil sorbent performance testing, *Journal of Testing and Evaluation,* 43, 1- 8 (2015).

35. Salleh M.A.M., Mahmoud D.K., Karim W.A.W.A, and Idris A., Cationic and anionic dye adsorption by agricultural solid wastes: A comprehensive review. *Desalination*, 280, 1-13(2003).

36. Rida K., Bouraoui S. and Hadnine S., Adsorption of methylene blue from aqueous solution by kaolin and zeolite. *Applied Clay Science*, 83.84, 99-105(2013).

37. Yang X.K., Omer A.M., Khalifa R.E., Zhaohong H. and Chao L., Fabrication of tetraethylenepentamine functionalized alginate beads for adsorptive removal of Cr (VI) from aqueous solutions, *International Journal of Biological Macromolecules,* 125, 1221-1231(2019).

38. Nandi B., Goswami A. and Purkait M., Removal of cationic dyes from aqueous solutions by kaolin: Kinetic and equilibrium studies. *Applied Clay Science*, 42(3-4), 583-590(2009).

39. Subinoy J., Efficient and selective removal of cationic organic dyes from their aqueous solutions by a nanocomposite hydrogel, katira gum-cl-poly (acrylic acid-co-N, N-dimethylacrylamide) bentonite, *Applied Clay Science*, 173, 46-64(2019).

40. Feng D., Bai B., Wang H. and Suo Y., Novel fabrication of PAA/PVA/yeast superabsorbent with interpenetrating polymer network for pH-dependent selective adsorption of dyes, *Journal of Polymers and the Environment,* 26 (2), 567-588(2018).

41. Abdel Ghafar H. H., Embaby M. A., Radwan E. K., Abdel-Aty A. M .,Biosorptive removal of basic dye methylene blue using raw and CaCl2 treated biomass of green microalga Scenedesmus obliquus, *Desalination and Water Treatment*, 81, 274–281(2017).

أزالة صبغة ازرق الميثيلين من المحاليل المائية بواسطة حمض الاكريليك المطعم مع بيوتيل ميث اكريلات الممغنط

راندا اصلاح خليفة خليفة غنيم[1]، أحمد غزلان[2]، حمادة عبد الوهاب[3]

[1] قسم بحوث المواد البوليمرية- معهد التكنولوجيا المتقدمة والمواد الجديدة- مدينة الأبحاث العلمية والتطبيقات التكنولوجية- مصر

[2] شركة رائد للصناعات الكيماوية ومستحضرات التجميل- مصر

[3] قسم الكيمياء- كليه العلوم - جامعه الأزهر-مصر

فى هذه الدراسة تم تحضير متراكب نانومغناطيسى من البولى أكريلك والميثيل ميثأكريلات عن طريق عملية البلمرة بتقنية الترسيب, لإزالة صبغة الميثلين الأزرق من مياه الصرف الصناعى. ولقد تم توصيف المادة المازة باستخدام أجهزة الأشعة تحت الحمراء والميكروسكوب الماسح الإلكترونى وتم أيضا قياس ثباتها الحرارى. كما تمت دراسة العديد من العوامل المؤثرة على كفائة عملية الإمتزاز مثل: زمن التلامس, الرقم الهيدروجينى لمحلول الصبغة, التركيز الإبتدائى للصبغة, كمية المادة المازة, وأيضا سرعة التقليب. ولقد أوضحت النتائج أن كفائة عملية الإمتزاز تقل مع زيادة التركيز الإبتدائى للصبغة بينما وجد أنها تزيد بزيادة معدل التقليب من 100 إلى 300 لفة فى الدقيقة. كما وجد أيضا بدراسة تأثير الرقم الهيدروجينى للصبغة المستخدمة أن أعلى نسبة إزالة للصبغة والتى تصل تقريبا إلى 98% قد سجلت عند pH 3.5. لذا فأن النتائج تظهر إمكانيه استخدام المتراكب النانومغناطيسى البولميرى بكفاءة تصل ل 100% كمادة مازة واعدة لأزالة صبغة الميثيلين الأزرق من المياه الملوثة.